Burner system for solid sample flame emission spectroscopy

Adam Bernicky,[a] Boyd Davis,[b] and Hans-Peter Loock[c*]

[a]Department of Chemistry, Queen's University, Kingston, ON, Canada
[b]Kingston Process Metallurgy, Kingston, ON, Canada
[c]Department of Chemistry, University of Victoria, Victoria, BC, Canada
* hploock@uvic.ca

Abstract

We present a burner system to analyze solid inflammable samples utilizing flame emission spectroscopy without requiring any sample preparation procedures. The acetylene-nitrous oxide burner was designed to efficiently introduce solid particles into the flame through active injection, enabling real-time elemental analysis. Computational Fluid Dynamics (CFD) simulations were employed to study particle transport dynamics within the burner system. The emission was characterized through spectral analysis of the flame emission from metal powder mixtures, demonstrating its ability to determine elemental compositions without prior sample treatment. An artificial neural network (ANN) was implemented to analyze spectral data obtained from binary metal mixtures, enabling rapid and reliable identification of constituent elements with an uncertainty of σ = 2.7 % (mol/mol_{total})

Introduction and motivation

Process control in primary copper manufacturing is practically non-existent. In the most common metallurgical process, copper is extracted from enriched copper sulphide-containing ores ("concentrates") by feeding the pulverized concentrates (particle size: 10-50 μm) into a flash furnace where the powder ignites, releasing SO_2. The condensed combustion products are collected at the bottom of the furnace where two liquid layers form. The copper-rich sulphide layer, the matte, and the slag layer containing iron-silicon oxides can then be separated.

Since the feedstock is constantly changing, supplementary oxygen and/or fuel (natural gas) must be added to the flame, and their fraction must frequently be adjusted to maintain optimal conversion of the feedstock to matte. Depending on the geographical source of the ore, the concentration of copper-bearing sulphide minerals which become matte, such as chalcopyrite (CuFeS), bornite (Cu_5FeS_4), covellite (CuS), and chalcocite (Cu_2S), frequently changes. Accordingly, the relative concentration of minerals that convert to slag, such as pyrite (FeS_2) and those that remain inert (SiO_2), also varies. Process control is currently limited by the difficulty of determining the feedstock composition in real-time. The mineralogical analysis is complicated since the environment is extremely hostile (high dust loading, high temperature), there is no opportunity for sample preparation, and the sample is heterogeneous.

While the feedstock composition can sometimes be inferred from the physical characteristics of the flame in the flash furnace, previous attempts to measure flame conditions in a flash furnace model were limited to blackbody temperature and brightness measurements of the flame.[1] Atomic emission from heavy elements such as copper and iron could not be used for concentration measurements due to insufficient thermal excitation.[2] Sensing systems for pyrometallurgical processes used fiber optic probes to monitor the flame within the flash furnace.[3-7] For example, in a recent study, the intensity of the flame emission, its

temperature from blackbody radiation[1], and some atomic and molecular information were obtained using air-cooled fiber-optic probes by applying principal component analysis (PCA) to the spectral datasets.[1]
Here, we demonstrate a sample analysis system based on the flame emission of a solid sample introduced directly into a high-temperature acetylene-nitrous oxide flame. The sample is gravity-fed with the help of a Venturi nozzle and contains either neat metal, known minerals, or concentrates obtained from a copper smelter. The flame emission spectra are recorded every few seconds and can be correlated to the composition of the concentrate, which is obtained using conventional methods.
We found that conventional spectroscopic analysis is complicated by the blackbody background and the many short-lived species in the flame. Inner-filter effects also complicate the extraction of quantitative information from band intensities. An Artificial Neural Network (ANN) algorithm, appropriately trained on known samples, provides a robust analysis of the concentrate composition. We previously demonstrated that the sample's elemental composition can be readily obtained with an accuracy of around 1-2% using a very basic acetylene burner.[8]
The paper is structured as follows. First, the background of solid sample flame emission systems is described before presenting the design of the burner and sample introduction system, followed by a determination of its most important characteristics. We demonstrate that the copper and iron concentrations of a solid sample relevant to the non-ferrous metallurgical industry can be obtained by neural network analysis of the emission spectra. Details on the artificial neural network analysis were presented previously,[8] and, here, we focus on the results that are most relevant to the characterization of the solid sample flame emission system. A detailed mineralogical analysis using a similar artificial neural network is presented in a companion report.

Background

Quantitative measurements of analytes via flame emission techniques were first published by Lundegådh in 1939, and commercial spectrophotometers were made available by Beckman[9] and others from 1950 onwards. Flame emission spectrometer systems frequently use acetylene, hydrogen, butane, propane, and/or natural gas as fuel and combinations of oxygen, air, or nitrous oxide as oxidizers. Oxygen:acetylene burners were operated in a total consumption configuration instead of a pre-mixed configuration to minimize the flashback risk, given the high flame front velocity.[10] Modern analytical burners are constructed of corrosion-resistant materials, such as stainless steel or titanium[11], and are routinely used for quantitative analysis of trace elements. In all commercial systems, solid samples need to be dissolved before the solution can be introduced into the flame. A sample solution is introduced into the flame using an atomization chamber that entrains aerosol droplets into the pre-mixed fuel/oxidant flow. Sometimes, the solutions must be filtered to ensure the atomizer is not clogged. Only very few reports describe injecting powdered materials *directly* into a flame, and some of those studies involved additional sample preparation processes, such as creating a suspension in an organic solvent before spraying.[12] Using solid powdered fuel is not impossible, however. In the 1960s, Edse et al. described the formation of a unique metal-oxygen flame. The metal-oxygen burner consisted of a pilot flame with a coaxial flow of metal powder and oxygen at a high flow rate.[13]
The specific requirements for the analysis of copper concentrates guided our design. The flame had to reach a high temperature of at least 2500 K and maintain the temperature for varying concentrations of sulphide-containing concentrates, i.e., from a sample that consists mainly of chalcopyrite and Cu-sulphides to samples that contain significant fractions of oxides, such as silica and iron oxides. The system must also entrain the sample particle stream in the flame for long enough so that the mineral sulphides are largely

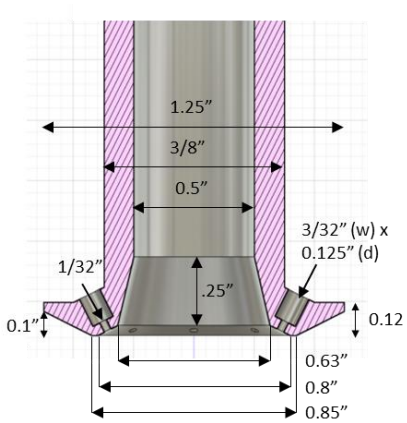

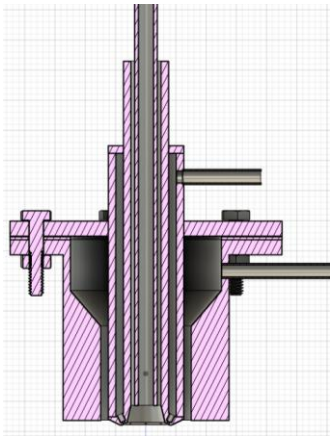

Figure 1: Schematic drawing of the burner. The inner body (left) and the fully assembled burner with mated flange (right).

Figure 2: Accumulation of powder on burner orifices was observed

converted and consumed. This is important since the particles may have a surface composition that differs from those of their interiors. The design chosen for the burner presented here is a hybrid of a high-temperature acetylene-oxidant flame and a solid fuel:oxidant flame. While the solid feed would sustain a flame by itself, the acetylene fuel is added to produce the high temperatures required to generate meaningful emission spectra. The burner has a coaxial design to ensure that the sample particle stream is engulfed by the flame until it is converted.

Several burner designs have been investigated in the course of our development.[14] We previously demonstrated a simple, horizontal acetylene-oxidant torch into which a powdered sample was fed by gravity.[8] Aside from its scale (the flame was 20-30 cm long) this resembles most closely the conventional “flame test” conducted for over 100 years using a Bunsen burner. We also investigated a vertical burner in which the pre-mixed gases are ignited when exiting eight nozzles, which are arranged in a circle around a larger central hole through which the sample is fed by gravity. This flat-faced burner was found to be wasteful of thermal energy and created a cool pocket where the sample would exit the burner face. Consumption of the solid fuel would only occur at some distance from the burner faceplate which varied with the shape of the rather unstable flame.[14]

Design of the Burner

Here, we present a burner that was built with an angled faceplate (Figure 1). The flame generated by the concentric angled burner was designed to engulf the feed material right when it exits the feed tube. The burner faceplate was constructed by machining the inner burner from a single piece of stainless steel (316 SS), thereby eliminating unnecessary welds. The bottom plate has an OD of 1.25” (31.8 mm), a shaft OD of ¾” (19.1 mm) and an ID of 0.5” (12.7 mm). Eight holes (3/32” × 0.125”; 2.38 × 3.18 mm) were drilled into the face plate’s surface (angled at 22.5º) and were countersunk with a 1/32” (0.80 mm) hole. A taper on the inner and outer portions of the piece prevents clogging. A tube (length: 4-3/8” (137 mm); ID: 1” (25.4 mm), OD: 1.25” (31.8mm)) was welded to the inner burner piece and capped with a 1/8” (3.175 mm) lid to contain the fuel gas. A flange (thickness: 3/8” (9.53 mm) thick; 4.5” (114 mm OD) with 5 equally spaced holes is also welded to the outer burner body 1-1/8” (35 mm) from the top of the outer body. An inlet using ¼” (6.35 mm) tubing is welded to burner between the top of the burner lid. A second flange to mate with the other flanged piece has a 2.5” (63.5 mm) opening that tapers down to 1.6” (40.6 mm) after 1” (25.4 mm) from the top. A hole is drilled in the straight section to attach a ¼” (6.35 mm) tube so that

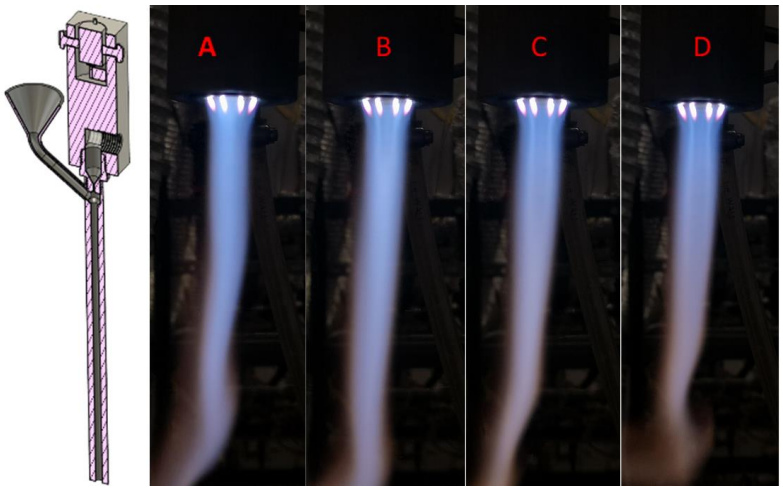

Figure 3: Design of Venturi powder injector (left) and evolution of injector feather with increasing flow of the central particle air stream from 0 L/min (A) to 0.5 L/min (B), 1 L/min (C), and 1.5 L/min (D).

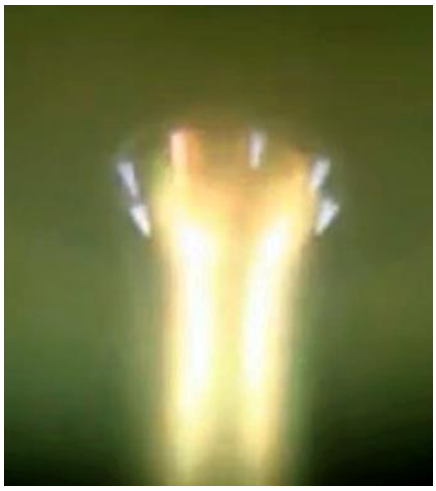

Figure 4: Flame emission when Cu-powder is fed into the flame

sheath gas can be directed around the burner body. The short distance between the eight adjacent, angled burner holes (0.31", 7.87 mm) effectively eliminated the cooler pockets and more efficiently directed the heat toward the central axis of the burner, where it is needed (Figure 3).

The burner was connected to a gas handling system, allowing for independent flow control of a variety of oxidant and fuel gases. Nitrous oxide was selected as the oxidant due to concerns related to the safety of acetylene-oxygen flames and their propensity to produce flashbacks at low flow velocities.[15] Additionally, the length of an acetylene-oxygen flame would be much longer than required. The acetylene-N_2O flame was approximately 10" (250 mm) long and initially 0.75" (20 mm) wide before narrowing to 0.5" (12 mm) within the first few centimetres (Figure 3). The very narrow flame is preferred over the much broader flame generated by a flat burner face since the coalescence of the eight initial flames into a single homogeneous flame (as opposed to a cylindrical flame) will ensure the flame fully envelops samples after exiting the central burner hole.

The performance of the prototype was benchmarked by injecting pure copper and iron metal powders by passive (gravity) injection. Compared to our previous burner designs the resulting emission was very bright (Figure 4) and only a small amount of material was required to produce useable emission intensities, which suggests that the angled burner is much better at consuming the entire sample quickly and completely compared to our previous designs.[14]

Venturi injector with vibrational mount

The transport of powder through the central feed cavity was facilitated with a powder Venturi injector (also referred to as a Venturi Eductor[16, 17]), which was designed to entrain powdered samples within a carrier gas stream. The injector forces the gas flow from an inlet tube (ID 3/8"; 9.525 mm) through a 0.03" (0.76 mm) diameter constriction before it again expands into the Venture feed tube (ID 3/8"). The Bernoulli equation gives the pressure differential which depends on the gas density, ρ, the flow velocity, Q, and the cross-sectional areas of the three tube sections.

$$p_{in} - p_{out} = \frac{\rho}{2}\left(v_{out}^2 - v_{in}^2\right) = \frac{Q^2\rho}{2}\left(A_{out}^{-2} - A_{in}^{-2}\right) \quad (1)$$

With (1) we calculate the pressure differential between the inlet tube (3/8" ID) and the 0.03" throat as 800 Pa (0.08 atm) for a flow velocity of Q = 1 L/min. The lower gas pressure at the exit of the Venturi constriction draws the sample powder from the feed line into the vertical tube.

The feedline and sample container were attached to an eccentric vibrational motor to improve mass transport and to ensure that the powder remains fluidized at the sample inlet. The Venturi injector shown in Figure 3 is coupled to the burner by inserting the Venturi feed tube (ID 3/8"; 9.53 mm) through a bored 3/8" -3/4" (9.53 – 19.1 mm) coupling such that the outlet of the Venturi tube was positioned 0.25" (6.35 mm) above the burner face plate (Figure 5).

We found that a carrier gas flow greater than Q = 1 L/min introduced turbulence and, therefore, unpredictable flame chemistry. It also produced a separate coaxial particle stream in the centre of the flame and nearly along its entire length, limiting the interaction of particles with the acetylene-oxidant flame (see Figure 3). The carrier gas flow was, therefore, set to 1 L/min or less.

A pre-mixed acetylene-nitrous oxide flame with mixing ratios of 1.25 L/min:3.50 L/min was ignited. Overheating of the burner is prevented by flowing ~15 L/min of sheath gas (compressed air) through an opening concentric with the outer burner body. Light emitted from the flame is collected by an armoured fibre optic cable (Thorlabs, 800 µm core diameter) that is connected to a ¼" optical port threaded to accept the SMA 905 connector. The length of the optical port limits the field of view to a circular area at the flame (Ø 5 mm) and reduces the effect of temperature gradients in the flame. The spectra reported here were obtained using 10 ms integration time. Since ten spectra were averaged, the effective acquisition rate was 10 averaged spectra per second.

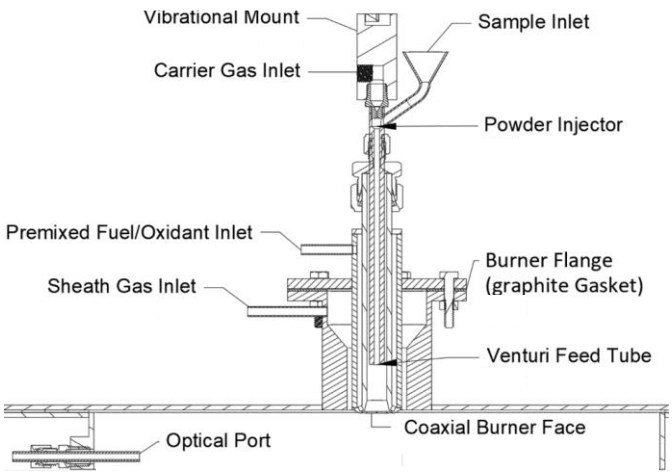

Figure 5: Schematic of the coaxial injection burner for solid phase emission spectroscopy.

Computational Fluid Dynamic (CFD) analysis

We observed that some material accumulated on the burner face near the eight burner holes when feeding mineral sulfide powders for analysis. The accumulation eventually resulted in blockages and asymmetric flames when left unabated. Occasional cleaning was required (see Figure 2).

To investigate the cause of the localized accumulation of material, a computerized fluid dynamic analysis model was generated by computer aided design based on the burner dimensions (Figure 1). The inlet flow for the fuel/oxidant inlet tube, the sheath gas flow, and the carrier gas flow were set to 4.75 L/min, 15 L/min, and 1 L/min, respectively. A single outlet was then set as the unknown so that the software (Autodesk CFD 2023, version 23.0) could determine the path of the gas.

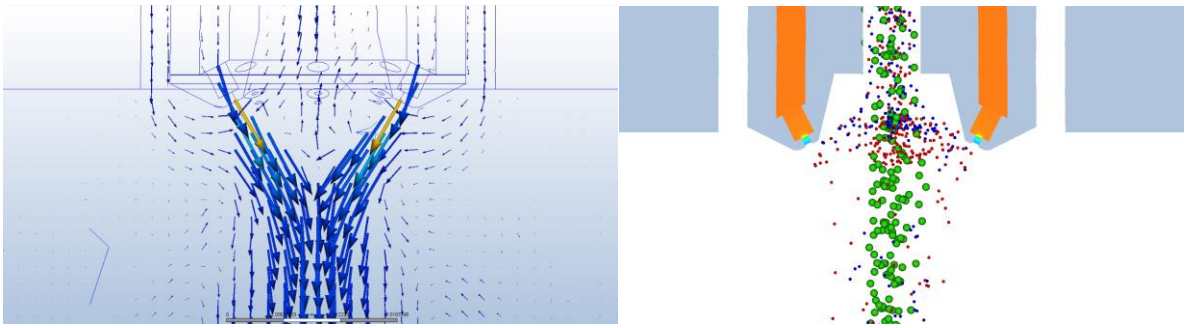

Figure 7: (left) Results of CFD analysis of the burner. A vector field indicates the flow of gas from the burner face. (right) A simulation of the injection of 10 (blue), 20 (red), and 30 µm (green) particles with a density equal to that of chalcopyrite

A vector field was generated to illustrate the flow of gases at the burner face (Figure 7). The vector field indicated a reversal of gas flow along the central axis to the inner wall of the burner. The high-velocity flow of pre-mixed fuel/oxidant creates an unintended Venturi effect that draws the particle stream from the central hole toward the burner holes. When the central gas flow was simulated to contain particles of different sizes having the density of chalcopyrite (Figure 7; right), it was found that the smallest particles are drawn to the perimeter of the feed tube, where they are pulled toward the low-pressure region created by the high-speed gas flow around the burner holes. A future design modification may include a constriction for the centre flow to achieve a higher particle flow velocity or to recede the burner holes into the burner face to reduce the pressure drop across the burner face.

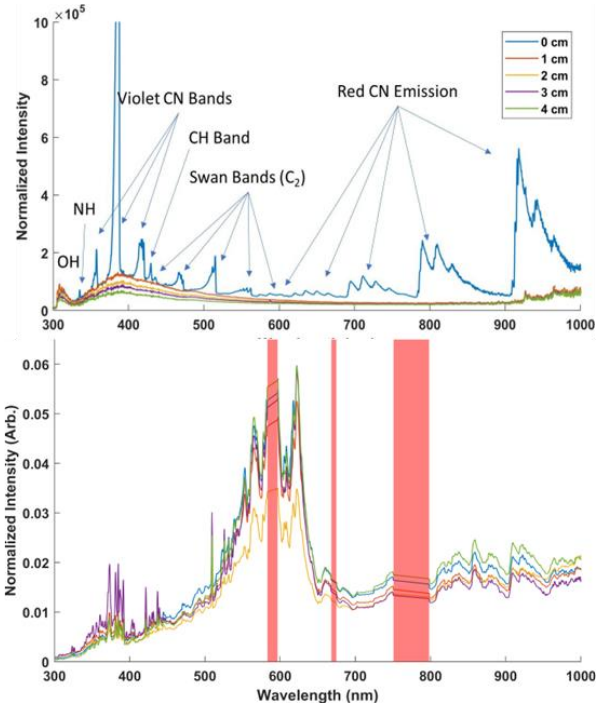

Figure 6: (Top) Emission spectrum of a partially combusted pre-mixed acetylene-nitrous oxide flame. Violet and red emission bands from cyano radical (CN) and dicarbon radical (C_2) dominate the emission spectrum. Emissions from methylidyne (CH), imidogen (NH), and hydroxyl radical (OH) are also indicated. (Bottom) Emission spectra of chalcopyrite collected at 1 cm intervals from the burner faces. Saturating Na, K, and Li atomic emission lines have been removed as indicated by the shaded pink areas.

Characterization of the flame emission system

The flame emission without solid feed was collected using the fiber-coupled spectrometer as described above. Averaged spectra from the pre-mixed acetylene-nitrous oxide flame were recorded at different distances from the burner faceplate (Figure 6; Top). The spectra at very short distances from the faceplate are dominated by the bright emission from the eight feathers, which contain numerous intermediate species indicative of incomplete combustion. They are readily assigned using previous reports.[18-22] At larger distances, the molecular bands disappear and the spectra only show a broad continuum, with a maximum near 380 nm that decreases in intensity with increasing distance from the burner plate.

When chalcopyrite powder is fed through the central hole, the emission is dominated by bright atomic and molecular species even at the burner faceplate (Figure 6; Bottom). Conveniently, the relative intensities of the spectral features do not change

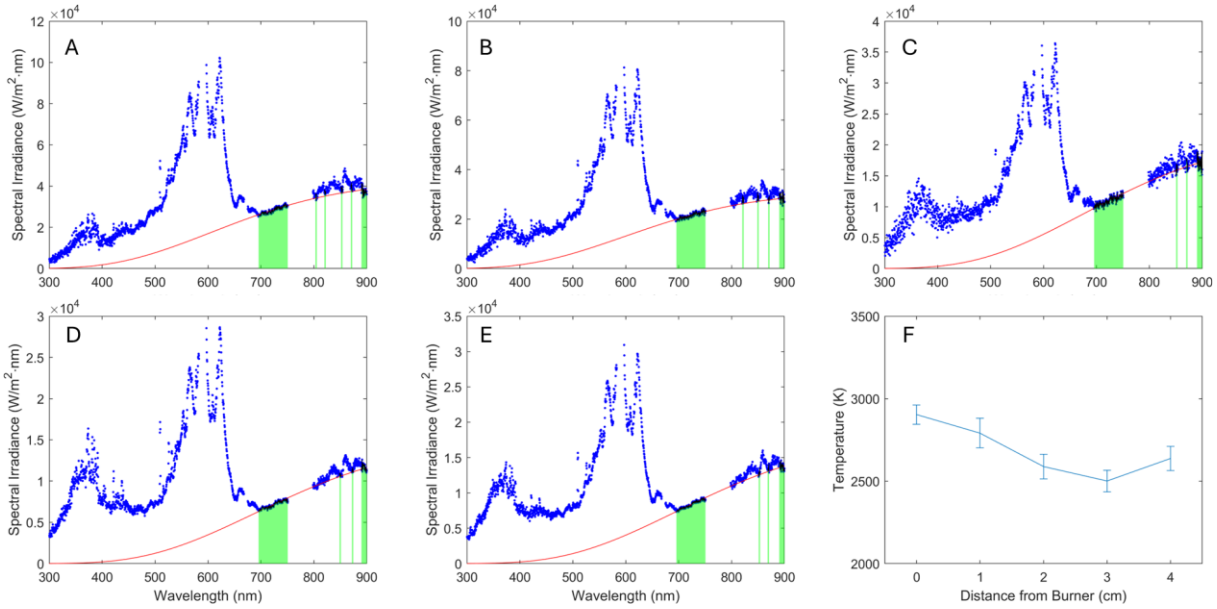

Figure 8: Emission spectra collected at 1 cm intervals from the burner face with fit to the blackbody emission curve from 0 cm (A) to 4 cm (E). Green bars indicate the spectral regions used for the fit. The average temperature obtained from the fit illustrates a slightly decreasing flame temperature with increased distance from the burner face (F).

much with distance. Strong atomic lines that are due to alkali earth constituents (Na, K, Li) were removed as indicated by the shaded pink sections in Figure 6.

Spectral regions without molecular and atomic lines can be used to determine the blackbody temperature from flames that contain particles. These spectral regions (indicated in green in Figure 8) were fit to a blackbody spectrum following calibration with a reference blackbody emitter.[23] The resulting temperature profile shows that the flame temperature decreases from 2850 ± 75 K near the burner to 2500 ± 75 K at 3-4 cm (Figure 8). For the experiments reported here, the spectra were sampled at around 3 cm (Figure 8: Emission spectra collected at 1 cm intervals from the burner face with fit to the blackbody emission curve from 0 cm (A) to 4 cm (E). Green bars indicate the spectral regions used for the fit. The average temperature obtained from the fit illustrates a slightly decreasing flame temperature with increased distance from the burner face (F).Figure 8D) from the faceplate to ensure a stable and high temperature and bright emission from the powdered sample.

Artificial Neural Network, ANN

In our previous work and in a companion publication, we elaborate on the use of ANNs in complex spectral analysis.[8] For the purpose of this study, we only demonstrate the principle of ANN analysis using over 800 spectra obtained by feeding eleven samples prepared by mechanically mixing two metallic powders - copper powder and iron powder (both *Sigma*, >99% metal basis).

A custom code was written in the MATLAB™ environment using its *Statistics and Machine Learning Toolbox* to randomly divide the spectral data set into training, validation, and testing subsets in a ratio specified by the user. As previously described, the training algorithm is based on a scaled gradient descent using the performance gradient of the validation subset.[8] A descriptor label is assigned to each measurement - here, each spectrum - based on the externally validated property.

In order to determine the required size and complexity of the model, our code starts by training a network without a hidden layer (k = 0) to obtain a baseline performance of the simplest ANN with the given number of input (i) and output nodes, n. The convergence criterion held to 5 validation failures to ensure

proper model generalization. The code then increases the complexity of the model by one hidden layer and then iteratively increases the number of nodes in this hidden layer until the hidden layer contains up to 400 nodes. The weights and biases of each ANN architecture are optimized iteratively, and the performance of the testing and validation subsets is determined for each epoch until a stopping criterion is met. This is also repeated 30 times to ensure the model's global minimum is obtained for a particular architecture. The performance trend is calculated to determine if a global minimum has been reached and to prevent unnecessary training. Specifically, the performance of the two most recent ANN architectures is compared to the third. If the most current version performs worse than the previous two architectures, the model stops increasing the number of nodes and proceeds to the next training phase. In the event two models with different convergence criteria and model sizes produce similar performance, the model with fewer total nodes is selected to minimize the computational load required for future applications since the number of weighted connections increases by $n(n_o+n_{out})+(k\text{-}1)n^2$ when $k\geq 1$ Next, the number of hidden layers is increased by one, and the process above is repeated.

For this simple binary Cu:Fe system, our custom ANN training algorithm converged with just a single hidden layer containing five nodes. Here, the dataset was normalized according to the Euclidean norm (2-norm).[24] The model achieved an excellent correlation to the expected descriptor values (Figure 9) with a root mean square error of $\sigma \approx 2.7\ \%_{mol}$ for the two metal concentrations and < 7 K for the flame blackbody temperature. The limits of detection were calculated using the 3σ confidence intervals of the correlation curves[25] and are found to be $15\%_{mol}$ for copper and iron. In a forthcoming publication we illustrate that more complex sample mixtures also require much more complex ANNs.

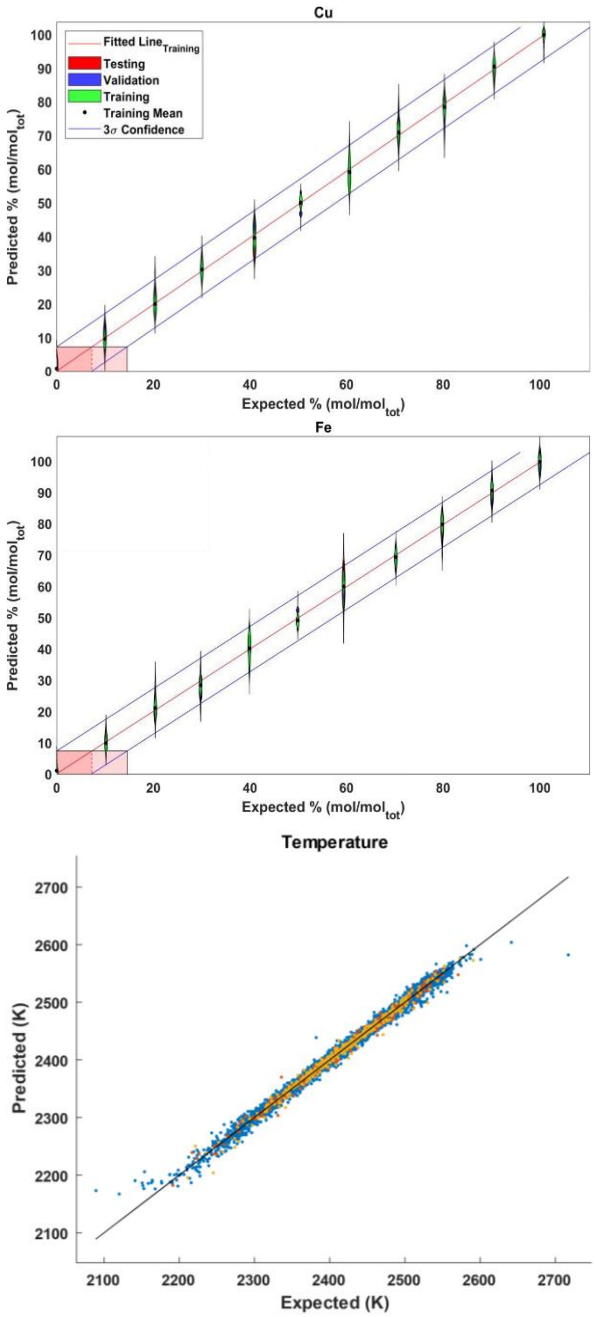

Figure 9: Violin correlation plots for copper (top) and iron (centre) descriptors with a distribution of ANN model error and LOD for the 2-norm normalization dataset. The LOD for copper and iron are 14% and 15%, respectively. The bottom panel shows the correlation between the temperature determined from a fit to the blackbody emission and that found using the ANN.

Conclusion

The direct introduction of solid inflammable samples into a novel burner system eliminates the need for sample preparation required by conventional instrumentation. An angled burner face, in combination with a sample introduction system, based on Venturi eductor, ensures the complete introduction of feed powders. Benchmark testing produced emission spectra rich with atomic and molecular emission features. The application of artificial neural networks to a spectral dataset produced from the analysis of binary mechanical mixtures of metal powders achieved an accuracy of 2.7 $\%_{mol}$ and a limit of detection of ~15 $\%_{mol}$. CFD calculations, including particle simulations, revealed that low-pressure areas at the burner face result in small-particle migration to the burner face where accumulation can occur.

Acknowledgements

AB thanks Alain Roy for many useful discussions, and Trevor LeBel, Maya Stricker, Chris Pelow, Kathy Golshani, Russell Dawes, and Mark Woodrow for their technical assistance and advice. HPL and AB are grateful to the Natural Science and Engineering Research Council (NSERC) of Canada for financial support under the Collaborative Research and Development Program. BD thanks the National Research Council of Canada Industrial Research Assistance Program (NRC IRAP) for financial support.

Conflict of Interest Statement

BD is the co-founder and Principal of Kingston Process Metallurgy Inc., a company which co-financed the present research.

References

(1) Stokreef, A. Measuring the Effect of Concentrate Mineralogy on Flash Furnace Smelting Using Drop Tower Testing and a Novel Optical Probe. Queen's University, 2018.
(2) Stokreef, A.; Barnes, J. A.; Loock, H.-P.; Davis, B. J. A. I. O. Fiber optic probe for process control in copper smelters. **2019**.
(3) Arias, L.; Torres, S.; Toro, C.; Balladares, E.; Parra, R.; Loeza, C.; Villagrán, C.; Coelho, P. Flash Smelting Copper Concentrates Spectral Emission Measurements. **2018**, *18* (7), 2009.
(4) Arias, L.; Balladares, E.; Parra, R.; Sbarbaro, D.; Torres, S. Sensors and Process Control in Copper Smelters: A Review of Current Systems and Some Opportunities. **2021**, *11* (1), 1.
(5) Myakalwar, A. K.; Sandoval, C.; Sepúlveda, B.; Fuentes, R.; Parra, R.; Balladares, E.; Vásquez, A.; Sbarbaro, D.; Yáñez, J. Laser induced breakdown spectroscopy for monitoring the molten phase desulfurization process of blister copper. *Analytica Chimica Acta* **2021**, *1178*, 338805.
(6) Vásquez, A.; Pérez, F.; Roa, M.; Sanhueza, I.; Rojas, H.; Parra, V.; Balladares, E.; Parra, R.; Torres, S. A Radiometric Technique for Monitoring the Desulfurization Process of Blister Copper. **2021**, *21* (3), 842.
(7) Yañez, J.; Torres, S.; Sbarbaro, D.; Parra, R.; Saavedra, C. Analytical instrumentation for copper pyrometallurgy: challenges and opportunities. *IFAC-PapersOnLine* **2018**, *51* (21), 251-256.
(8) Bernicky, A.; Davis, B.; Barnes, J.; Loock, H.-P. Spectroscopic characterisation of feedstock for copper smelters by machine-learning. *Canadian Metallurgical Quarterly* **2023**, 1-10.
(9) Gilbert, P. T.; Hawes, R. C.; Beckman, A. O. Beckman Flame Spectrophotometer. *Analytical Chemistry* **1950**, *22* (6), 772-780.
(10) Kniseley, R. N.; D'Silva, A. P.; Fassel, V. A. A Sensitive Premixed Oxyacetylene Atomizer-Burner for Flame Emission and Absorption Spectroscopy. *Analytical Chemistry* **1963**, *35* (7), 910-911.
(11) Elmer, P. *AAnalyst 400 AA Spectrometer*; 2010.
(12) Gilbert, P. T., Jr. Direct Flame-Photometric Analysis of Powdered Materials. *Analytical Chemistry* **1962**, *34* (8), 1025-1026.
(13) Edse, R.; Rao, K. N.; Strauss, W. A.; Mickelson, M. E. Emission Spectra Excited in Metal Powder–Oxygen Flames*. *J. Opt. Soc. Am.* **1963**, *53* (4), 436-438.
(14) Bernicky, A. R. Through the Fire and Flames: Characterization of Solid Samples with Flame Emission Spectroscopy and Artificial Neural Networks. Queen's University, 2024.
(15) Aldous, K. M.; Bailey, B. W.; Rankin, J. M. Burning velocity of the premixed nitrous-oxide/acetylene flame and its influence on burner design. *Analytical Chemistry* **1972**, *44* (1), 191-194.
(16) Eductors, F. V. Case Study #43 - Fox Ceramic-Lined Eductors for Conveying Abrasives.

(17) Pneuvay. *Venturi Eductors And Jet Pumps In Pneumatic Conveying Systems*. 2023. https://www.pneuvay.com.au/pneumatic-conveying/news/Venturi-eductors-and-jet-pumps-in-pneumatic-conveying-systems/ (accessed May 2024).
(18) Bayes, K. D. A Study Of CN Emission From Active Nitrogen Flames. *Canadian Journal of Chemistry-Revue Canadienne De Chimie* **1961**, *39* (5), 1074-&.
(19) Nicholls, R. W. Franck-Condon Factors To High Vibrational Quantum Numbers 3 - CN. *Journal of Research of the National Bureau of Standards Section a-Physics and Chemistry* **1964**, *A 68* (1), 75-+.
(20) Fox, J. G.; Herzberg, G. Analysis of a new band system of the C₂ molecule. *Physical Review* **1937**, *52* (6), 0638-0643.
(21) Gaydon, A. *The Spectroscopy of Flames*; Springer Dordrecht, 1974. DOI: https://doi.org/10.1007/978-94-009-5720-6.
(22) Huber, K. P.; Herzberg, G. *Molecular Spectra and Molecular Structure: IV Constants of Diatomic Molecules*; Litton Educational Publishing,Inc., 1979.
(23) Jones, H. A. A Temperature Scale for Tungsten. *Physical Review* **1926**, *28* (1), 202-207.
(24) Mathworks. Norms: Vector and Matrix Norms. 2023.
(25) Loock, H.-P.; Wentzell, P. D. Detection limits of chemical sensors: Applications and misapplications. *Sensors and Actuators B: Chemical* **2012**, *173*, 157-163.